35th Annual International Conference of the IEEE EMBS
Osaka, Japan, 3 - 7 July, 2013

Influence of isotropic skull models on EEG source localization

Victoria Montes-Restrepo, Pieter van Mierlo, José D. López, Hans Hallez and Stefaan Vandenberghe

Abstract— **We investigated the influence of using simplified skull models on electroencephalogram (EEG) source localization. The simplified skull models were derived from CT and MR images, with isotropic conductivity modeled as either heterogeneous or homogeneous. A total of four simplified head models were compared against a reference model with a skull accurately segmented with CT images. Our results show that the use of a simplified geometry for the skull, can lead to errors of approximately 1 cm for sources located in the central and temporal regions of the brain.**

I. Introduction

The localization of neural activity using the electroencephalogram (EEG) relies on an accurate model representing the human head. In this model, the skull plays an important role due to its low conductivity compared to the other tissues inside the head. In addition, the skull has an inhomogeneous structure, consisting of spongy and compact bone as well as air-filled cavities.

Although magnetic resonance imaging (MR) is the most common technique for the visualization of the structure of the head, the geometry of the skull cannot be easily distinguished from these images. In contrast, computed tomography (CT) allows for the correct visualization of the skull and its different tissue types but it is not frequently performed on patients due to the ionizing radiation. Therefore, the accurate segmentation of the geometry of the skull remains unresolved.

The skull has often been modeled as an isotropic compartment due to its simplicity and feasibility of being incorporated in forward solutions based on spherical and boundary element methods [1]. However, the inhomogeneities of the skull generate an anisotropic conductivity throughout its structure. Even though anisotropic conductivity modeling of the skull has been used in multiple applications [2]–[4], its calculation requires the use of tensors for each voxel which severely increases the computation time. Additionally, some authors [5], [6] did not find a significant improvement when using anisotropy and instead recommended to model the skull as a heterogeneous isotropic compartment.

In this work, we analyze the influence of using simplified skull models with isotropic conductivity on EEG source localization. A head model with a skull segmented from CT images is incorporated in the analysis as ground truth and used for the forward model solution. Using the CT-based geometry, two models with either homogeneous or heterogeneous isotropic conductivity are generated. The same procedure is followed for a skull geometry segmented from MR images. In this way, four head models are generated for the computation of the inverse problem. Moreover, we investigate in which brain region the error is highly affected by using the simplified skull models. This can be done by simulation studies with a parametric dipole model where the reference dipoles are placed on a regular grid over the gray matter tissue.

This work was supported by iMinds (Interdisciplinary Institute for Technology), Belgium

V. Montes-Restrepo, P. van Mierlo and S. Vandenberghe are with Faculty of Engineering, MEDISIP, iMinds, Ghent University, 9000 Ghent, Belgium (e-mails: {victoria.montesrestrepo, pieter.vanmierlo}@ugent.be)

J. D. López is with Department of Electronic Engineering, Universidad de Antioquia, Medellín, Colombia (e-mail: josedavid@udea.edu.co)

H. Hallez is with the Faculty of Engineering Technology, Reliability in Mechatronics and ICT, Catholic University College of Bruges-Ostend (KHBO), 8400 Oostende, Belgium (e-mail: hans.hallez@khbo.be)

II. Methods

A. Head model generation

Different realistic head models were generated using the MR and CT images of one patient from the database of the reference center of epilepsy of the Department of Neurology at the Ghent University Hospital (Belgium). The T1-weighted MR images were acquired using a 3T scanner (Siemens Trio, Erlangen, Germany) and consisted of a $256 \times 256 \times 176$ matrix with voxel size 0.86 mm $\times$ 0.86 mm $\times$ 0.9 mm. These images were used to segment the scalp and brain tissues. The scalp was segmented through thresholding followed by a closing with hole filling operation. The segmentation of cerebrospinal fluid (CSF), white matter (WM) and gray matter (GM) was done with the SPM8 software package [7].

The CT images (Toshiba Aquilion, Tokyo, Japan), coregistered with the MR, were used to accurately segment the skull. A CT/MR thresholding approach followed by morphological operations such as dilation and erosion were performed in order to obtain the skull compartment. The thickness of the skull was kept within the normal limits for an adult skull, with maximal thickness of 7 mm in the occipital region [8]. The generated head models are explained as follows:

1) Reference model: In order to perform a comparison between the models, a *reference* or *ground truth* is established. This reference head model incorporates a realistic geometry for the skull, consisting of separate isotropic layers for the compact and spongy bone compartments in addition to air-filled cavities such as the frontal and sphenoidal sinuses. This model is presented in Fig. 1 and Table I.

2) Model 1 – Isotropic heterogeneous skull (layCT): The skull is modeled as a heterogeneous compartment, but the spongy layer is not segmented directly from the CT image. It is constructed by iteratively eroding the compact layer six times with a $3 \times 3 \times 3$ cross-shaped structuring element, until

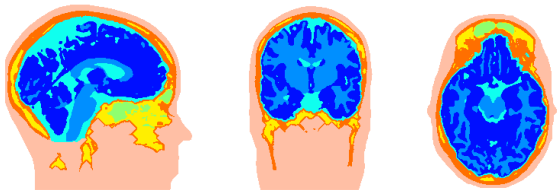

Fig. 1: Reference head model in sagittal, coronal and axial views, showing seven different tissue types: Scalp, CSF, WM and GM segmented from MR; Compact bone, Spongy bone and Air cavities, all segmented from CT.

TABLE I: Conductivities for the reference head model.

Tissue	Conductivity (S/m)	
Scalp	0.3279	[9]
Compact bone	0.0064	[10], [11]
Spongy bone	0.02865	[10], [11]
Air cavities	0.0000	[12]
Cerebrospinal Fluid	1.7857	[13]
White Matter	0.1428	[12]
Gray Matter	0.3333	[12]

its thickness in the occipital region is below 3 mm [8]. Thus, it is an approximation of the actual layered structure of the skull, that is useful when the skull geometry is accurate but the spongy bone cannot be distinguished.

3) Model 2 – Isotropic homogeneous skull (isoCT): The skull is modeled as a homogeneous isotropic compartment with air cavities.

4) Model 3 – Isotropic heterogeneous skull (layMR): This model incorporates separate layers for the spongy and compact bone, all segmented from the MR image. A skull mask is extracted from the MR image using the SPM toolbox. This mask is overlaid with the original MR image and the resulting image is thresholded in order to distinguish between spongy and compact bone.

5) Model 4 – Isotropic homogeneous skull (isoMR): The skull is modeled as a homogeneous isotropic compartment with air cavities, with the geometry segmented from the MR image.

Table II summarizes the analyzed skull models and shows the skull conductivities σ in each case.

B. EEG source localization

Once the head models are constructed, the EEG source localization problem can be solved, which requires solving a forward and an inverse problem. Solving the forward problem, the electrode potentials at the scalp caused by a dipolar source are obtained. In this study, we used 128 electrode positions that were based on the 10/5 system [18]. The electrode potentials caused by a dipole at $\mathbf{r}$ with orientation $\mathbf{d}$ can be written as

$$\mathbf{V}_{model}(\mathbf{r},\mathbf{d}) = \mathbf{L}(\mathbf{r}) \cdot \mathbf{d} \qquad (1)$$

TABLE II: Summary of the different skull models analyzed. For models 1 and 2, the skull was segmented from CT images while models 3 and 4 incorporate a skull segmented from MR. Model 1 uses a spongy layer that corresponds to an erosion of the compact bone.

Model		Tissue	Segmentation	σ (S/m)
Ref		Compact	CT	0.0064
		Spongy	CT	0.02865
		Air cavities	CT	0.0000
1		Compact	CT	0.0064
		Spongy	eroded compact	0.02865
		Air cavities	CT	0.0000
2		Compact + Spongy	CT	0.0105
		Air cavities	CT	0.0000
3		Compact	MR	0.0064
		Spongy	MR	0.02865
		Air cavities	MR	0.0000
4		Compact + Spongy	MR	0.0105
		Air cavities	MR	0.0000

where $\mathbf{V}_{model} \in \mathbb{R}^{128\times 1}$ are the calculated electrode potentials at one instance, and $\mathbf{L}(\mathbf{r}) \in \mathbb{R}^{128\times 3}$ is the lead-field matrix, which is dependent on the dipole location, the head model geometry, the conductivities and the electrode positions. The calculation of the forward problem in this study is done with the *finite difference method* (FDM) with reciprocity [16] that can incorporate anisotropies (AFDRM) [15]. The calculation grid of the AFDRM consisted of 5,745,427 nodes. The time required to compute the forward matrix using 128 electrodes was approximately 3 hours per electrode pair using one core of a CPU dual-socket quad-core Intel Xeon L5520 (Intel Nehalem microarchitecture, 2.27 GHz, 8 MB L3 cache per quad-core chip). Due to the use of isotropic layers, the difference in computational complexity between the models is not noticeable. However, for the models with three-layered skull, the complexity is slightly higher than for models with a single compartment skull.

The *inverse problem* is defined as the estimation of the dipole parameters ($\mathbf{r}$,$\mathbf{d}$) that best fit a surface potential ($\mathbf{V}_{in}$). This is done by the minimization of the relative residual energy (RRE) [15]:

$$RRE = \frac{\|\mathbf{V}_{in} - \mathbf{V}_{model}(\mathbf{r},\mathbf{d})\|_2^2}{\|\mathbf{V}_{in}\|_2^2} + \mathbf{C}(\mathbf{r}) \qquad (2)$$

where $\mathbf{V}_{in}$ is the set of given electrode potentials and $\mathbf{V}_{model}(\mathbf{r},\mathbf{d})$ is the set of electrode potentials calculated by solving the forward problem in models 1 to 4, respectively. The term $\mathbf{C}(\mathbf{r})$ is a penalization parameter that restricts the search space to the brain compartment, being zero when the dipole is located inside the brain (gray and white matter) and large otherwise. The minimization is performed with the Nelder-Mead simplex method.

C. Experimental setup

We investigated the dipole localization errors due to using a simplified head model (model i, $\forall i \in 1,2,3,4$) instead of a

more realistic one (reference model) in the dipole estimation.

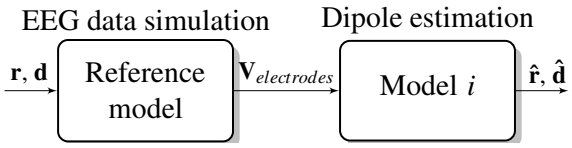

Fig. 2: Simulation setup used to compare the reference model with the simplified head models (model i, $\forall i \in 1,2,3,4$).

Test dipoles were placed on a 3D grid with distance of 5 mm between each node. Only the nodes situated in the gray matter were considered, resulting in a total of 6904 dipoles. Three orthogonal orientations were considered for each dipole location according to the Cartesian coordinate system: X–, Y– and Z–orientation.

For each test dipole with parameters $\mathbf{r}$ and $\mathbf{d}$, the electrode potentials were calculated by solving the forward problem using the reference model. In this way, the simulated noiseless EEG data at the electrodes was obtained.

Subsequently, from the simulated noiseless potentials $\mathbf{V}_{electrodes}$, the dipoles were estimated by solving the inverse problem using models 1 to 4. Using the simulation setup displayed in Fig. 2, we investigated the dipole location errors due to simplifications in the conductivity modeling of the skull (Models 1 and 2 vs. Reference) and in the skull geometry (Models 3 and 4 vs. Reference).

Hence, the error due to the use of a simplified model in the solution of the inverse problem was investigated. The set of dipole parameters $\hat{\mathbf{r}}$ and $\hat{\mathbf{d}}$ that minimizes the cost function, are the estimated dipole parameters in the simplified head model.

The dipole localization error (DLE) was evaluated through the Euclidean distance between the original dipole location $\mathbf{r}$ and the estimated dipole location $\hat{\mathbf{r}}$:

$$\text{DLE} = \|\hat{\mathbf{r}} - \mathbf{r}\|$$

In order to investigate which regions of the brain are more affected by the use of a simplified skull, the mean DLEs for the frontal, central (cingulate cortex) and temporal lobes were computed.

III. Results

Fig. 3 shows the dipole localization errors for models 1 to 4. The DLEs for Model 1, Fig. 3a, are larger for deep sources in the brain than for superficial ones. There is asymmetry towards the right side of the brain due to the differences in spongy bone between Model 1 and the reference model. For Model 2, Fig. 3b, the localization errors are larger in the temporal and superior parietal regions of the brain.

Localization errors for models 3 and 4 are large in the basal and bottom regions of the brain. For Model 3, Fig. 3c, the errors for the superficial sources distributed along the cranial vault are small. Model 4, Fig. 3d, exhibits large errors at the base but less extended, and in the cranial vault the errors are in general larger than for Model 3.

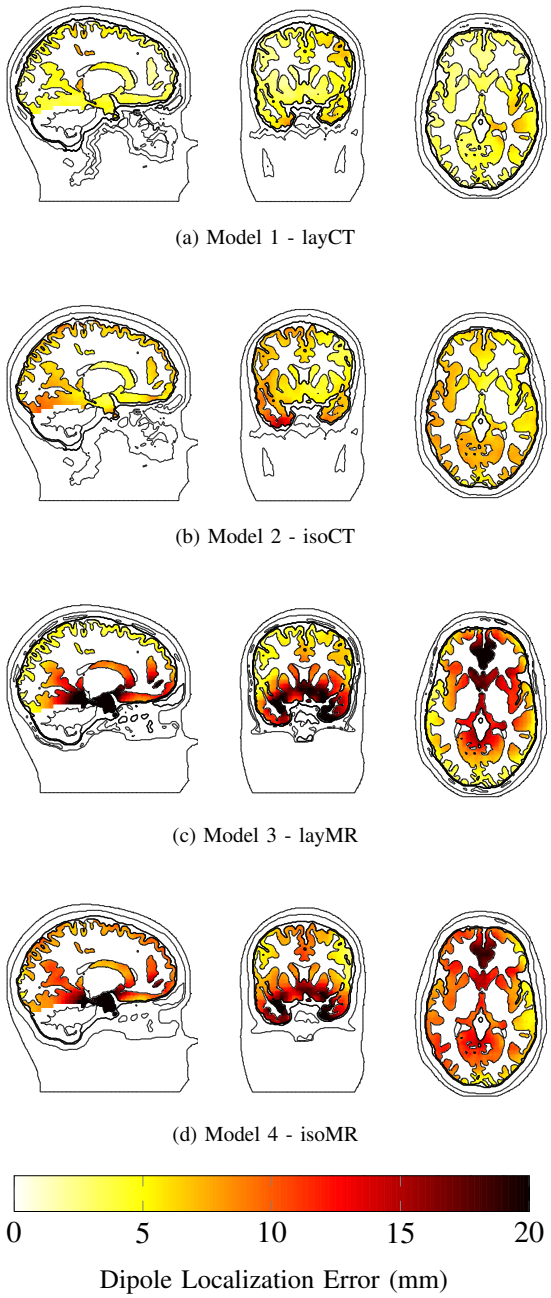

(a) Model 1 - layCT

(b) Model 2 - isoCT

(c) Model 3 - layMR

(d) Model 4 - isoMR

Fig. 3: Dipole localization errors for models 1 to 4.

The mean DLEs for frontal, cingulate and temporal lobes in the brain are displayed in Fig. 4. The largest difference between CT- and MR-based models is obtained in the central region (cingulate cortex), i.e., for deep sources in the brain. For the frontal lobe, there is not such a large difference due to the similarity between MR and CT images in this region. In the temporal lobe, there is a significant difference between the CT- and MR-based models. However, for MR-based models there is not a noticeable inter-modality variability for the cingulate and temporal lobes.

We did not take into account the influence of noise for the simulations performed in this work. This because we

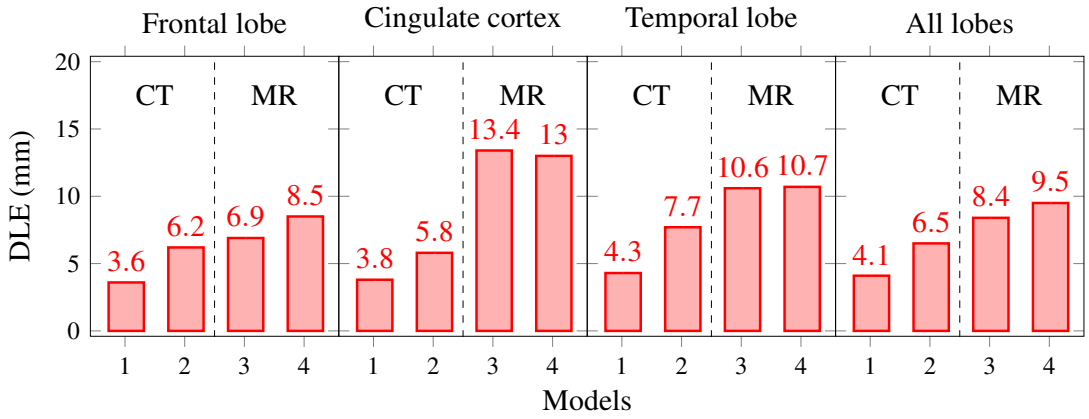

Fig. 4: Mean localization error for different lobes of the brain.

investigated the error due to simplifications of the model, and adding noise would probably affect the inverse solutions, preventing to differentiate anatomical effects among models. Posterior studies will be performed specifically for determining the noise effects.

IV. Conclusions

In this paper CT- and MR-based skull models have been studied and compared. When CT-based skull models were used, the lowest errors were obtained with a heterogeneous isotropic compartment, with the spongy bone modeled as an erosion of the compact bone. This model can be used when the spongy bone cannot be easily segmented but the geometry of the skull is accurate.

For the MR-based skull models, there were large errors for the sources located near the basal region of the brain, due to the larger difference in geometry between these and the CT-based models.

Modeling the skull as a homogeneous isotropic compartment introduced errors in the cranial vault and temporal regions of the brain.

V. Acknowledgments

The authors gratefully acknowledge Radiology and Neurology Department of the Ghent University Hospital for providing the patient data used in this study. The computational resources (Stevin Supercomputer Infrastructure) and services used in this work were provided by Ghent University, the Hercules Foundation and the Flemish Government - department EWI.

References

[1] M. Stenroos and J. Sarvas, "Bioelectromagnetic forward problem: isolated source approach revis(it)ed," *Physics in Medicine and Biology*, vol. 57, no. 11, p. 3517, 2012.

[2] G. Marin, C. Guerin, S. Baillet, L. Garnero, and G. Meunier, "Influence of skull anisotropy for the forward and inverse problem in EEG: simulation studies using FEM on realistic head models," *Human Brain Mapping*, vol. 6, no. 4, pp. 250–269, 1998.

[3] C. Wolters, A. Anwander, X. Tricoche, D. Weinstein, M. Koch, and R. MacLeod, "Influence of tissue conductivity anisotropy on EEG/MEG field and return current computation in a realistic head model: A simulation and visualization study using high-resolution finite element modeling," *NeuroImage*, vol. 30, no. 3, pp. 813–826, 2006.

[4] H. Hallez, S. Staelens, and I. Lemahieu, "Dipole estimation errors due to not incorporating anisotropic conductivities in realistic head models for EEG source analysis," *Physics in Medicine and Biology*, vol. 54, pp. 6079–6093, 2009.

[5] R. Sadleir and A. Argibay, "Modeling skull electrical properties," *Annals of Biomedical engineering*, vol. 35, no. 10, pp. 1699–1712, 2007.

[6] M. Dannhauer, B. Lanfer, C. Wolters, and T. Knösche, "Modeling of the human skull in EEG source analysis," *Human Brain Mapping*, vol. 32, no. 9, pp. 1383–1399, 2011.

[7] K. Friston, Ed., *Statistical parametric mapping: The Analysis of Functional Brain Images*. Academic Press Inc., U. S., 2006.

[8] N. Lynnerup, J. Astrup, B. Sejrsen *et al.*, "Thickness of the human cranial diploe in relation to age, sex and general body build," *Head & Face Medicine*, vol. 1, no. 13, 2005.

[9] S. Gonçalves, J. de Munck, J. Verbunt, F. Bijma, R. Heethaar, and F. Lopes da Silva, "In vivo measurement of the brain and skull resistivities using an EIT-based method and realistic models for the head," *IEEE Transactions on Biomedical Engineering*, vol. 50, no. 6, pp. 754–767, 2003.

[10] M. Akhtari, H. Bryant, A. Mamelak, E. Flynn, L. Heller, J. Shih, M. Mandelkern, A. Matlachov, D. Ranken, E. Best *et al.*, "Conductivities of three-layer live human skull," *Brain Topography*, vol. 14, no. 3, pp. 151–167, 2002.

[11] M. Fuchs, M. Wagner, and J. Kastner, "Development of volume conductor and source models to localize epileptic foci," *Journal of Clinical Neurophysiology*, vol. 24, no. 2, pp. 101–119, 2007.

[12] J. Haueisen, C. Ramon, P. Czapski, and M. Eiselt, "On the influence of volume currents and extended sources on neuromagnetic fields: A simulation study," *Annals of Biomedical Engineering*, vol. 23, no. 6, pp. 728–739, 1995.

[13] S. Baumann, D. Wozny, S. Kelly, and F. Meno, "The electrical conductivity of human cerebrospinal fluid at body temperature," *IEEE Transactions on Biomedical Engineering*, vol. 44, no. 3, pp. 220–223, 1997.

[14] J. Sarvas, "Basic mathematical and electromagnetic concepts of the biomagnetic inverse problem," *Physics in Medicine and Biology*, vol. 32, pp. 11–22, 1987.

[15] H. Hallez, B. Vanrumste, P. Hese, Y. D'Asseler, I. Lemahieu, and R. Walle, "A finite difference method with reciprocity used to incorporate anisotropy in electroencephalogram dipole source localization," *Physics in Medicine and Biology*, vol. 50, pp. 3787–3806, 2005.

[16] B. Vanrumste, G. Van Hoey, R. Van de Walle, M. D'Havè, I. Lemahieu, and P. Boon, "The validation of the finite difference method and reciprocity for solving the inverse problem in EEG dipole source analysis," *Brain Topography*, vol. 14, no. 2, pp. 83–92, 2001.

[17] H. Hallez, B. Vanrumste, P. Hese, S. Delputte, and I. Lemahieu, "Dipole estimation errors due to differences in modeling anisotropic conductivities in realistic head models for EEG source analysis," *Physics in Medicine and Biology*, vol. 53, pp. 1877–1894, 2008.

[18] R. Oostenveld and P. Praamstra, "The five percent electrode system for high-resolution EEG and ERP measurements," *Clinical Neurophysiology*, vol. 112, no. 4, pp. 713–719, 2001.